Carbohydrate Polymers 96 (2013) 163–171

Contents lists available at SciVerse ScienceDirect

Carbohydrate Polymers

journal homepage: www.elsevier.com/locate/carbpol

Influence of the extraction process on the rheological and structural properties of agars

Ana M.M. Sousa[a], João Borges[b], A. Fernando Silva[b], Maria P. Gonçalves[a,*]

[a] REQUIMTE, Faculdade de Engenharia, Universidade do Porto, Rua Dr. Roberto Frias, 4200-465 Porto, Portugal
[b] Centro de Investigação em Química (CIQ-L4), Departamento de Química e Bioquímica, Faculdade de Ciências, Universidade do Porto, Rua do Campo Alegre 687, 4169-007 Porto, Portugal

ARTICLE INFO

Article history:
Received 8 October 2012
Received in revised form 20 March 2013
Accepted 23 March 2013
Available online 29 March 2013

Keywords:
Microwave-assisted extraction
Traditional hot-water extraction
Rheology
AFM
cryoSEM

ABSTRACT

Agars obtained by traditional hot-water (TWE) and microwave-assisted (MAE) extractions were compared in terms of their rheological and physicochemical properties and molecular self-association in solutions of low (0.05%, w/w) and high (1.5%, w/w) polymer concentrations. At low concentration, thin gelled layers were imaged by AFM. Slow or rapid cooling of the solutions influenced structure formation. In each case, TWE and MAE agar structures were different and apparently larger for MAE. At high concentration, progressive structural reinforcement was seen; while TWE agar showed a more open and irregular 3D network, MAE agar gel imaged by cryoSEM was denser and fairly uniform. The rheological (higher thermal stability and consistency) and mechanical (higher gel strength) behaviors of MAE agar seemed consistent with a positive effect of molecular mass and 3,6-anhydro-α-L-galactose content. MAE produced non-degraded agar comparable with commercial ones and if properly monitored, could be a promising alternative to TWE.

1. Introduction

In recent years, the application of non-conventional energy sources in the extraction of natural compounds has gained great interest. Microwave-assisted extraction (MAE), which promotes the simultaneous heating of the whole sample matrix by using microwave irradiation, has been successfully applied in the extraction of a wide variety of natural products (Chan, Yusoff, Ngoh, & Kung, 2011; Fishman, Chau, Cooke, & Hotchkiss, 2008; Perino-Issartier, Abert-Vian, & Chemat, 2011; Santana, Ferrera, & Rodriguez, 2005). The use of specialized microwave systems as opposed to the classical domestic devices many times used in the past by researchers, allowed the proper control of vital operational parameters such as pressure and temperature, thus becoming of great interest for the industries. MAE advantages include drastic reduction of extraction times, higher recoveries, lower energy and solvent consumptions and reduced byproduct formation (Belanger & Paré, 2006; Leonelli & Mason, 2010; Srogi, 2006). Very recently, our group applied, for the first time, the MAE technique to the isolation of agar (Sousa, Alves, Morais, Delerue-Matos, & Gonçalves, 2010; Sousa et al., 2012), a gelling polysaccharide of great commercial value (Selby & Whistler, 1993). This previous research showed that agars with better gelling properties could be extracted when using MAE instead of the conventional extraction route (*i.e.* traditional hot-water extraction, TWE; Villanueva, Sousa, Gonçalves, Nilsson, & Hilliou, 2010).

Agar is ideally based on the neutral polysaccharide agarose, built up from 3-linked β-D-galactose and 4-linked 3,6-anhydro-α-L-galactose (3,6-AG) repeating units and responsible for the polymer's gelling character. Commonly, the anhydride bridge is absent and several substitution groups are observed throughout agar's backbone. This non-gelling polysaccharide is globally named agaropectin and comprises the charged fraction of the polymer (Matsuhashi, 1990). Agar gelation is believed to result from a two steps mechanism: a conformational transition (coil-to-helix) upon cooling an agar aqueous solution where the molecules are homogeneously distributed and interhelical aggregation, at temperatures below the polymer gelation point (Arnott et al., 1974; Clark & Ross-Murphy, 1987; Labropoulos, Niesz, Danforth, & Kevrekidis, 2002a; Nordqvist & Vilgis, 2011). When sufficient polymer concentration is reached, a 3D network (*i.e.* macroscopic gel) is formed while insufficient concentration will result in local aggregates, networks and/or individual molecules (Morris, Kirby, & Gunning, 2010). While agarose forms rigid polymeric networks, the sulfate ester groups present in the agaropectin fraction of agar cause kinks in the perfect alignment of the helices, thus leading to the formation of less compact structures (Labropoulos et al., 2002a). Several research papers have aimed at investigating the behavior of gel-forming polysaccharides in aqueous media by atomic force microscopy (AFM;

* Corresponding author. Tel.: +351 22 5081684; fax: +351 22 5081449.
E-mail addresses: anamsousa@fe.up.pt (A.M.M. Sousa), jborges@fc.up.pt (J. Borges), afssilva@fc.up.pt (A.F. Silva), pilarg@fe.up.pt (M.P. Gonçalves).

0144-8617/$ – see front matter © 2013 Elsevier Ltd. All rights reserved.
http://dx.doi.org/10.1016/j.carbpol.2013.03.070

e.g. Ikeda, Morris, & Nishinari, 2001; Noda et al., 2008; Roesch, Cox, Compton, Happek, & Corredig, 2004). Only two AFM studies of agarose have been reported (Maaloum, Pernodet, & Tinland, 1998; Pernodet, Maaloum, & Tinland, 1997) neither focusing on dilute solutions. However, cryogenic scanning electron microscopy (cryoSEM; *e.g.* Nordqvist & Vilgis, 2011; Tuvikene et al., 2008) and rheological (Labropoulos et al., 2002a; Labropoulos, Niesz, Danforth, & Kevrekidis, 2002b; Mohammed, Hember, Richardson, & Morris, 1998) studies of agarose gels seem well documented in the literature. Also, to the best of our knowledge, no imaging or rheological studies have been published comparing agars obtained by TWE and MAE.

The aim of the present work was to compare agars extracted using conventional (thermal heat; TWE) and non-conventional (microwaves; MAE) energy sources. The viscoelastic behavior of both polysaccharides was monitored through rheological measurements and relevant physicochemical properties typically associated with agar quality were determined. A commercial agar, extracted with thermal heat, was also characterized to better infer the quality of the extracted samples. AFM and cryoSEM techniques were used to image the molecular associations of MAE and TWE agars in solutions of, respectively, low and high polymer concentrations. Wild *Gracilaria vermiculophylla* from Ria de Aveiro, northwestern Portugal, was used as raw-material and optimal conditions described in previous reports were applied (Sousa et al., 2010; Villanueva et al., 2010).

2. Materials and methods

2.1. Algae collection and sample preparation

G. vermiculophylla was collected in Ria de Aveiro, northwestern Portugal (40°38″N, 8°43″W), during January 2011. The location and month of collection as well as the sample preparation were similar to those described in a previous work (Villanueva et al., 2010).

2.2. Agar extraction

Agar traditional hot-water (TWE) and microwave-assisted (MAE) extractions were performed according to previously optimized procedures (Villanueva et al., 2010; Sousa et al., 2010). A MARS-X 1500 W (Microwave Accelerated Reaction System for Extraction and Digestion, CEM, Mathews, NC, USA) apparatus with a maximum power output and a batch system of fourteen sealed Teflon® vessels was used for agar MAE process. The optimal conditions used in the TWE method were: 2 h at 85 °C under conventional heating, 200 mL of solvent and without agitation (Villanueva et al., 2010) while the optimized MAE conditions were: 5 min at 90 °C under microwave heating, 20 mL of solvent, with maximum stirring (Sousa et al., 2010). The extracts were purified and their water content estimated as described in Sousa et al. (2012). A commercial agar sample from Sigma–Aldrich (A-7002) was used as reference.

2.3. Preparation of agar solutions with low concentration

Dilute agar aqueous solutions of 0.05% (w/w) (*ca.* 500 μg/mL) concentration were prepared for AFM studies following two different procedures. The first one consisted in dispersing the appropriate polysaccharide amount in distilled water under vigorous stirring. The dispersions were then heated at ~96 °C for one hour and the resulting solutions were left to slowly cool to room temperature ('*slow cooling*' method). The other adopted procedure consisted in diluting with cold distilled water the concentrated solutions (1.5% (w/w); see Section 2.4) while hot (*i.e.* random coil state), to a final concentration of 500 μg/mL ('*fast cooling*' method). The pH of the solutions fell in the range ~6.4–6.7.

2.4. Preparation of agar solutions and gels with high concentration

Concentrated agar aqueous solutions were prepared by dispersing the appropriate amount of polysaccharide in distilled water under vigorous stirring and heating at ~96 °C for one hour. Approximately fifteen grams of the hot 1.5% (w/w) (*ca.* 1.5% g/mL) solutions were transferred to a cylindrical container with 30 mm diameter and properly covered to avoid water evaporation. The agar gels were left to set at room temperature and to equilibrate for 20 h. The gel depths were approximately 21–22 mm. The remaining hot agar solutions were used in the oscillatory rheological measurements.

2.5. Atomic force microscopy (AFM) imaging

AFM studies were performed in air at room temperature using a PicoLe Atomic Force Microscope (Molecular Imaging, USA) operating in dynamic tip deflection mode (Acoustic Alternating Current mode, AAC). Aliquots (25 μL) of each low concentration agar solution, prepared as described in Section 2.3, were deposited onto freshly cleaved discs of mica (Muscovite V-4, 15 mm diameter), allowed to dry in air for about 20 min, washed thoroughly with Millipore water, dried under a stream of nitrogen, and imaged by AFM in the tapping mode. Silicon cantilever (ACT-50, AppNano, USA) with a tip (pyramidal shape) height in the range of 14–16 μm, radius of curvature (ROC) lower than 10 nm, spring constant of 25–75 N/m, and a typical resonance frequency in the range 200–400 kHz was used for these purposes. Several areas of the mica surface were scanned in topography, amplitude, and phase modes with a resolution of 512 × 512 pixels and are representative of 5 μm × 5 μm regions over different locations on the studied mica surfaces. AFM images were corrected for bow/tilt by a second-order flattening using the PicoView™ 1.8.2 software (Agilent Technologies). The free Gwyddion 2.22 software was used to obtain the AFM parameters such as average root-mean-square surface roughness (R_{ms}) and the average heights (H_{av}) of the structures observed in Figs. 1 and 2, as well as the height profiles represented underneath the same images.

2.6. Penetration tests of agar gels

The gel strength (GS; g cm^{-2}), defined as the stress required for breaking the gel surface, was obtained from the force-deformation data measured in penetration tests, using a texture analyzer (Stable Micro Systems model TA-XT2, Surrey, England). Tests were performed at room temperature using a cylindrical plunger with 10 mm diameter attached to the equipment, operating at a penetration rate of 0.2 mm s^{-1}. Three replicates were performed for each agar gel.

2.7. Oscillatory rheological measurements

Dynamic rheological measurements were performed in a stress-controlled rheometer (ARG2, TA Instruments, USA) following a procedure described elsewhere (Sousa et al., 2010) with some improvements. A cone-and-plate geometry (4 cm diameter, 2° angle and a 54 μm gap) was used in all the determinations. The hot agar 1.5% (w/w) solutions (prepared in Section 2.4) were kept above 80 °C until the beginning of the experiment. The samples were covered with a layer of paraffin oil to prevent evaporation after having been placed into the measuring device, pre-heated at 80 °C. After an equilibration time of 10 minutes, the cooling step for gel formation

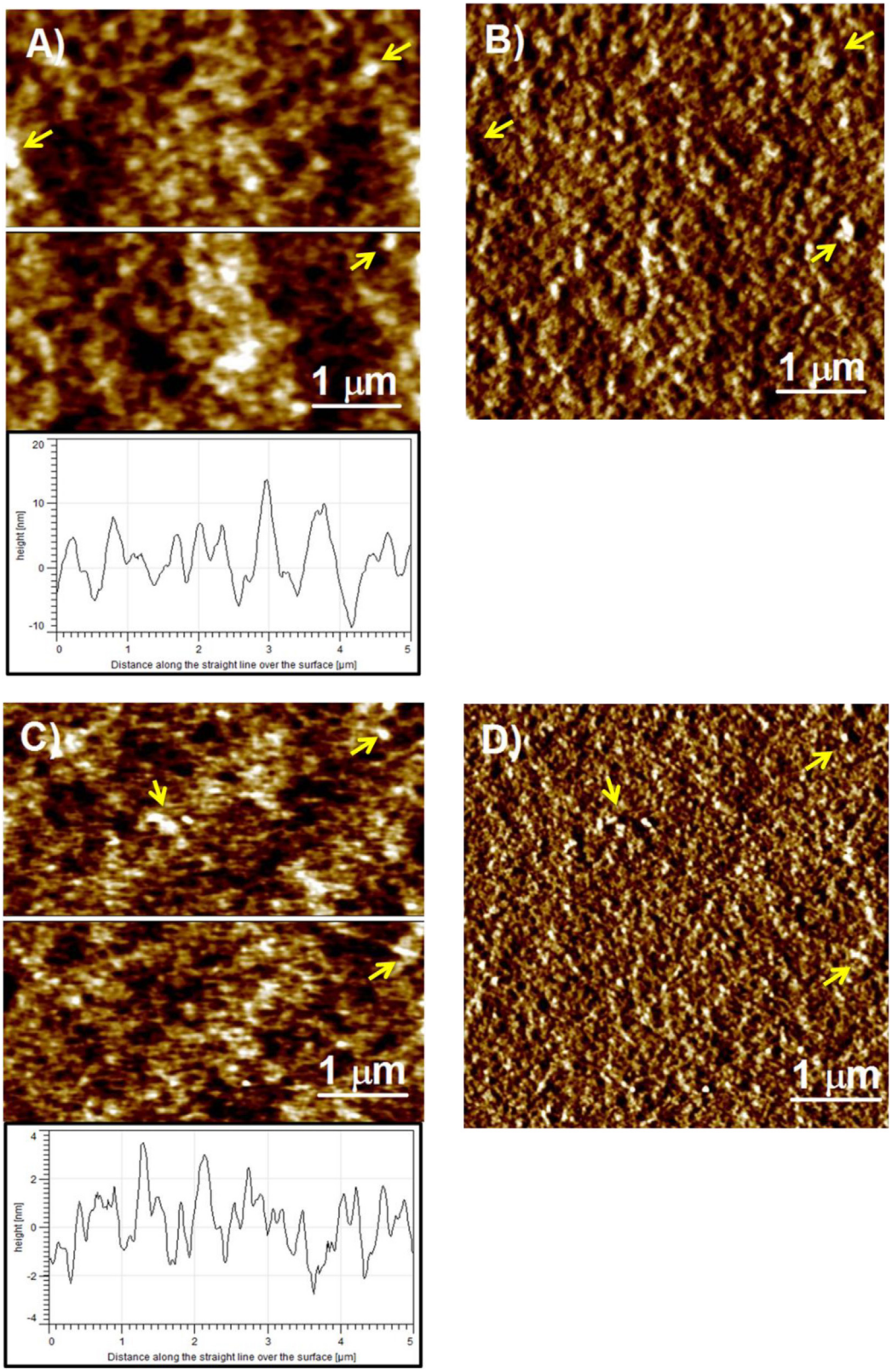

Fig. 1. Representative topographic (A and C) and equivalent amplitude (B and D) AFM images obtained in *tapping mode* for 0.05% (w/w) *ca.* 500 μg/mL aqueous solutions of MAE (A and B) and TWE (C and D) agars, prepared by the '*slow cooling*' method, deposited onto freshly cleaved mica after being cooled to room temperature. The image size is 5 μm × 5 μm. The curves below the images represent the height profile along the white line drawn in the images. Arrows indicate local aggregates.

was performed at a constant rate of 1 °C/min and at a fixed frequency of 1 Hz (6.28 rad/s) from 80 to 25 °C (at 1% strain amplitude). The gelation temperature (T_g) was defined as the crossover point of the elastic (G') and viscous (G'') moduli (*i.e.* when the loss tangent of the phase angle, tan δ, equals 1). However, it is important to have in mind that this criterion is rather simplistic if one considers the kinetic nature of the agar gelation process (Mohammed et al., 1998). Nonetheless, this concept works quite well for the purpose

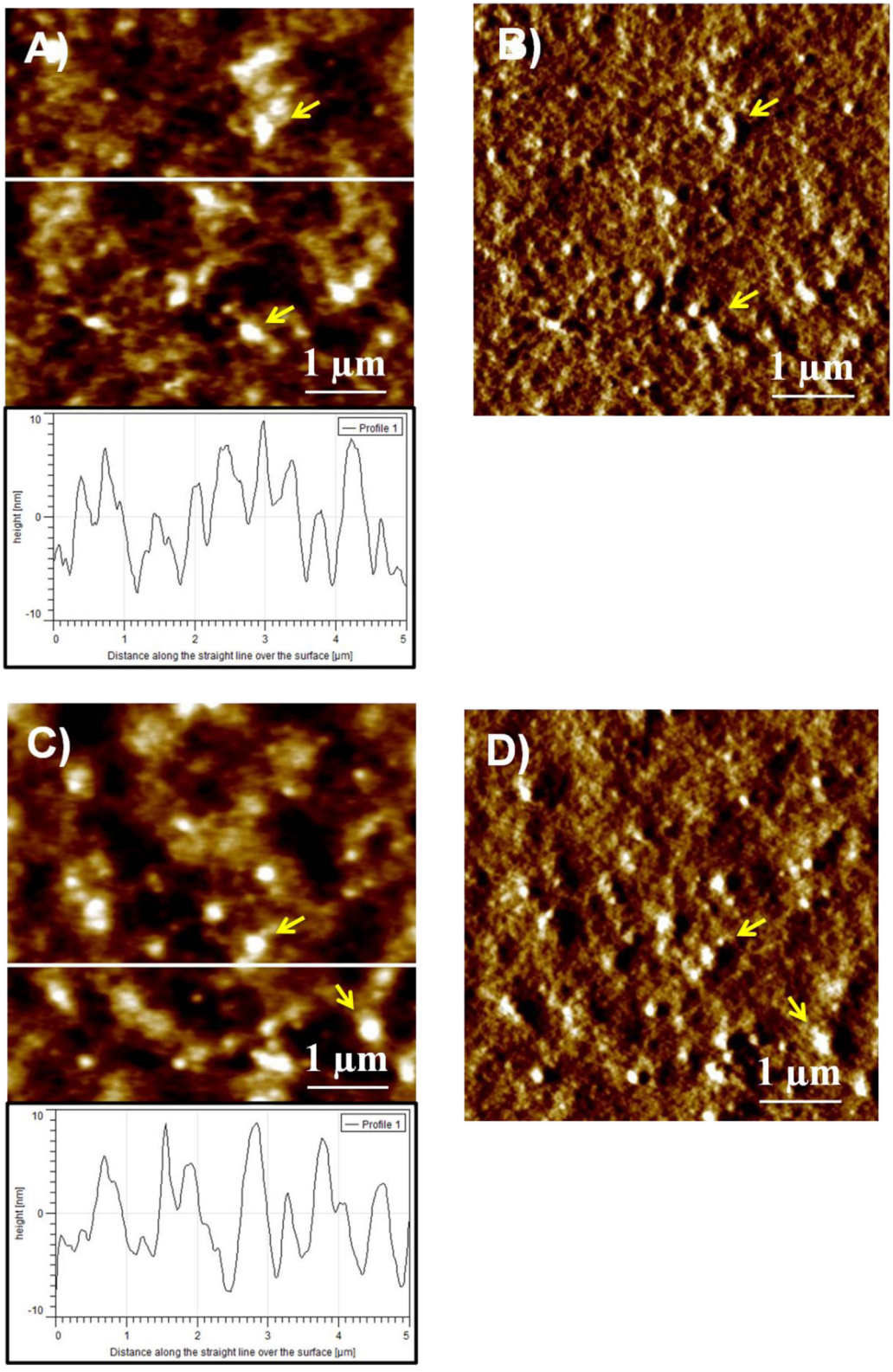

Fig. 2. Representative topographic (A and C) and equivalent amplitude (B and D) AFM images obtained in *tapping mode* for 0.05% (w/w) *ca.* 500 μg/mL aqueous solutions of MAE (A and B) and TWE (C and D) agars. The samples were deposited onto freshly cleaved mica after diluting while hot a 1.5% (w/w) agar solution ('*rapid cooling*' method). The image size is 5 μm × 5 μm. The curves below the images represent the height profile along the white line drawn in the images. Arrows indicate local aggregates.

of the present work. Gels were left to equilibrate at 25 °C before recording frequency sweeps (mechanical spectra) over the range 0.05–100 rad/s at 1% strain amplitude. Finally, the gel–sol transition was examined by submitting the samples to a heating step from 25 to 95 °C at a constant rate of 0.1 °C/min, at 1% strain amplitude and at a fixed frequency of 6.28 rad/s. The melting temperature (T_m) was determined according to the same criterion used to estimate agars' gelation point (*i.e.* tan $\delta = 1$) and the thermal hysteresis ($\triangle T$) was

Table 1
Physical and chemical properties of MAE and TWE agars extracted from *Gracilaria vermiculophylla*. Commercial agar was used as reference.

Properties	MAE agar	TWE agar	Commercial agar
GS (g cm^{-2})	1319 ± 53	1027 ± 46	1177 ± 43
M_v (kDa)[a]	136 ± 4	73.7 ± 2	138 ± 1
T_g (°C)	42.3 ± 0.2	40.9 ± 0.5	38.9 ± 0.3
T_m (°C)	89.7 ± 1.7	76.9 ± 1.7	92.1 ± 0.7
$\triangle T$ (°C)	46.8 ± 1.7	36.0 ± 1.1	53.1 ± 1.0
tan $\delta \times 10^2$[b]	1.84 ± 0.13	1.67 ± 0.07	2.09 ± 0.76
G_0 (kPa)[b]	25.6 ± 2.6	16.9 ± 2.0	33.9 ± 2.0
SO_3^- (%)[c]	2.5 ± 0.2	2.8 ± 0.1	1.6 ± 0.3
3,6-AG (%)[c]	40.7 ± 1.1	33.1 ± 1.6	43.5 ± 0.9
Water content (%)	13.2	13.1	12.9

[a] Determined from Mark Houwink equation, $[\eta] = 0.07 M_v^{0.72}$ (Rochas & Lahaye, 1989) as described in Sousa et al. (2012) and Souza et al. (2012).
[b] Average values (three replications) from mechanical spectra at 25 °C for 6.28 rad/s.
[c] Obtained as described in Sousa et al. (2012).

determined as $T_m - T_g$. All measurements were performed at least three times. The first order approximation of the Kronig–Kramers relations (Eq. (1)) proposed by Tschoegl (1989),

$$G'' = \frac{\pi}{2}\frac{d(G'(\omega))}{dln(\omega)} \quad (1)$$

was used to calculate $G''(\omega)$ from $G'(\omega)$ data and check if the frequency-sweep experiments were performed in the linear viscoelastic region (Sittikijyothin, Sampaio, & Gonçalves, 2007).

The relationship between the magnitude of the dynamic complex viscosity, $|\eta^*|$, and the frequency, ω, was determined using the power law equation (Eq. (2))

$$\left|\eta^*\right| = K\omega^n \quad (2)$$

where

$$\left|\eta^*\right| = \frac{\left(G'^2 + G''^2\right)^{1/2}}{\omega} \quad (3)$$

K is the dynamic consistency index and n the dynamic power-law factor. For completely elastic or completely viscous systems n equals −1 and 0, respectively (Noda et al., 2008).

2.8. Cryogenic scanning electron microscopy (cryoSEM) imaging

cryoSEM studies on 1.5% (w/w) agar gels were carried out at CEMUP (*Centro de Materiais da Universidade do Porto*) Porto, Portugal. The analyses were performed at −150 °C in a JEOL JSM 6301F scanning electron microscope equipped with a Gatan ALTO 2500 cryo preparation chamber using an accelerating voltage of 15 kV and working distances of 15 mm.

Approximately 1–3 mm^3 gel volume was placed in the sample holder and plunged in a nitrogen slush (−210 °C) to rapidly cool the sample. After freezing, the sample was transferred to an ALTO 2500 cryo preparation chamber and placed onto a cool stage (−150 °C), where it was fractured exposing the internal surface. The ice formed on the exposed fractured gel surface was removed by sublimation at −90 °C for 1.5 min. Finally, the sample was coated with sputtered Au–Pd thin film at −150 °C for 40 s, from a sputter head using ultrapure argon gas and was ready for the analysis.

3. Results and discussion

3.1. Physical and chemical properties of MAE and TWE agars

The physicochemical properties of agars extracted using conventional (TWE and commercial) and non-conventional (MAE) energy sources are given in Table 1. The gel strength (GS), a reference parameter of agar quality (Matsuhashi, 1990), was significantly higher for MAE agar (1319 ± 53 g cm^{-2} against 1027 ± 46 g cm^{-2} for the TWE polysaccharide). Nonetheless, both GS values fulfilled the market requirements for high-grade agars (GS > 700 g cm^{-2} at 1.5%, w/w) (Armisen, 1995). In addition, the GS of MAE agar compared favorably with that of the reference sample (1177 ± 43 g cm^{-2}) which clearly reveals the potential of MAE technique for the recovery of high-quality agars. The above results also show that *G. vermiculophylla* from Ria de Aveiro can be envisaged as a good and cheap raw-material for the agar industry, and replace *Gelidium* species (known for better quality agars) in specific applications (Armisen & Galatas, 1987).

Despite the dramatic acceleration of extraction observed when using MAE, the right choice of the operational parameters (5 min, 90 °C, 20 mL, with maximum stirring speed) allowed the recovery of agars with high molecular mass ($M_v \sim 138$ kDa), determined by viscometry (Sousa et al., 2012; Souza, Sousa, Gomez, & Gonçalves, 2012). The longer exposure of the extraction mixture to thermal heating in TWE (2 h, 85 °C, 200 mL, and without agitation; Villanueva et al., 2010) seemed to promote the degradation of the polymeric chains which explains the low $M_v \sim 73.7$ kDa (Hurtado-Ponce, 1992; Lai & Lii, 1998). In this context, the extraction of agars based on non-conventional energy sources such as microwaves can be a good strategy to obtain non-degraded agars under relatively mild processing conditions while significantly reducing the extraction times. The molecular mass, in turn, decreased in accordance with the polymer GS. This positive relation has been reported previously (Lai & Lii, 1998; Murano, 1995; Romero, Villanueva, & Montano, 2008), although within certain limits beyond which either the parameters become independent of molecular mass (upper limit) or the agar gelation does not take place (lower limit) (Murano, 1995). MAE agar showed significantly higher 3,6-AG fraction (~41%) than TWE agar (~33%) while the sulfate content was comparable (~2.7%). Therefore, in this case, the gelling ability of the polysaccharides seemed mainly governed by the molecular mass and the 3,6-AG content. In the following sections the rheological properties as well as the molecular organization of the polysaccharides in solutions and gels will be tentatively related with these two main properties. Overall, MAE agar showed comparable physical and chemical properties to the commercial sample used as reference.

3.2. AFM studies of low concentration agar solutions

Atomic force microscopy (AFM) was used to image MAE and TWE agars in aqueous solutions with low polymer concentration (500 μg/mL, *ca.* 0.05%, w/w). The samples were either slowly cooled to room temperature or rapidly quenched by dilution as described in Section 2.3. At room temperature, none of the prepared solutions formed macroscopic gels readily visible to the naked eye. In each case, the agar systems were then deposited onto freshly cleaved mica and air-dried.

Despite the amount and richness of information one can obtain when imaging gel-forming polysaccharides by the AFM technique, attention should be given to a couple of points. The first concerns the structural modifications that will most likely occur during the drying step when preparing the sample for analysis (Ikeda et al., 2001; Morris et al., 2010; Noda et al., 2008). The other relevant aspect is the difficulty to observe '*true solutions*' (Morris et al., 2010); very often, AFM images of such polysaccharides show large aggregates of intensively associated molecules caused by an insufficient solubilization of the polymer during the solution preparation and/or formed upon drying of the solution on the mica surface (Ikeda, Nitta, Temsiripong, Pongsawatmanit, & Nishinari, 2004;

Morris et al., 2010). To minimize this problem the agar powders were dispersed in the solvent under a vigorous vortex stirring and the dispersions were heated at high temperatures (~96 °C) until a homogeneous solution was obtained.

Fig. 1 shows the topographic and equivalent amplitude AFM images of the MAE (Fig. 1A and B) and TWE (Fig. 1C and D) agar solutions, when prepared by the '*slow cooling*' method. The images were acquired at a scanning size of 5 μm × 5 μm. For the considered conditions, both polysaccharides formed thin gelled layers on the mica surface (Fig. 1). Since the samples were deposited onto the substrate as liquids, the formation of the gels probably occurred as result of a substantial concentration increase upon drying of the samples (Ikeda et al., 2004). The height profiles illustrated below Fig. 1A (MAE agar) and 1C (TWE agar) seemed in line with this view; even if some compression should result in underestimated measured heights (Morris et al., 2010), the obtained values were higher (MAE agar typically ~5–10 nm and TWE agar ~1–3.5 nm) than expected for single agar molecules (Arnott et al., 1974). According to Arnott and co-workers each agarose chain with an average molecular weight of 120,000 is expected to form a three-fold helix of 1.9 nm pitch with an axial translation of 0.95 nm. Despite the evident massive aggregation state, it was clear that the structures formed by the two agar extracts were different and seemed considerably larger in the case of the MAE sample. In both cases, spherical and more rarely odd-shape aggregates (indicated with arrows) could be seen occasionally, buried in the polymeric networks, reaching greater dimensions in the case of MAE agar. Similar gelled structures were reported by Roesch et al. (2004) when imaging κ-carrageenan by AFM.

When diluting the 1.5% (w/w) agar solutions while hot, different structures were imaged by AFM (Fig. 2). Again, no discrete fibers were recognizable in the acquired images and polymeric gelled layers covered the mica surface. The distribution of heights illustrated below Fig. 2A and C seemed to support this interpretation (typically ~5–10 nm for both agars). The aggregates (indicated by arrows in Fig. 2) seemed more frequent than for slowly cooled agar solutions (Fig. 1) and were mainly spherical.

Differences between the two agar extracts were more difficult to establish. Values of surface roughness (R_{ms}) and average height (H_{av}) were derived from Figs. 1A and 2A (MAE agar) and Figs. 1C and 2C (TWE agar). Rapid cooling (Fig. 2) lead to surfaces with similar roughness (R_{ms} = 4.51 and 4.60 nm for MAE and TWE agars, respectively), but when the solutions were allowed to cool slowly (Fig. 1) a significantly smoother surface was formed by the TWE sample (R_{ms} = 1.13 nm, in comparison with 4.26 nm for the MAE extract). An identical trend was observed for H_{av} data (not shown). Although we were tempted to suggest that the structures in Fig. 2 were less organized than when slowly cooled (Fig. 1), the concentration used makes this interpretation purely speculative. However, one should expect that rapid quenching by dilution would decrease the interhelical association (Ikeda et al., 2001; Roesch et al., 2004), thus forming less organized structures than when slowly cooling the agar solutions. Mohammed and co-workers found that the formation of agarose gels was deeply affected by the cooling rate, suggesting that slow cooling promoted more aggregation of double helices than rapid quenching (Mohammed et al., 1998). Nonetheless, based only on the present AFM data, it seems reasonable to say that the systems formed by each polysaccharide were different and that MAE agar showed, apparently, larger structures than TWE agar, particularly when the solutions were cooled slowly.

3.3. Rheological studies of high concentration agar solutions/gels

In order to further understand the sol–gel transition of MAE, TWE and commercial agars, the elastic (G') and viscous (G'') moduli dependence on temperature of 1.5% (w/w) agar solutions was recorded at 1 °C/min from 80 to 25 °C. The gelation temperature (T_g) was considered as the crossover point between the two moduli (*i.e.* tan $\delta = G''/G' = 1$). For the sake of clarity, only G' and G'' data of MAE and TWE agars are shown in Fig. 3 (main graphic) while the tan δ data of the three samples are compared in the inset graphic of Fig. 3. The agar gelation occurred gradually, the sol–gel transition happening in a broad temperature window (~43–30 °C) and the shape of the curves was identical for MAE and TWE agars. Similar curves (not shown) were obtained for the commercial agar, but the transition started later in the cooling process (~40 °C).

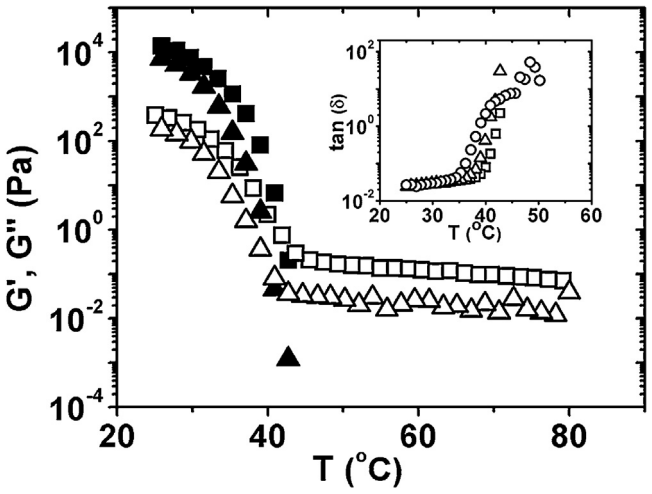

Fig. 3. Temperature dependence of elastic (G'; filled symbols) and viscous (G''; open symbols) moduli of 1.5% (w/w) agar sols/gels during cooling ramp from 80 to 25 °C (MAE (■, □) and TWE (▲, △) agars). Inset figure: temperature dependence of the loss tangent of 1.5% (w/w) agar sols/gels during cooling ramp from 80 to 25 °C (MAE (□), TWE (△) and commercial (○) agars). The measurements were recorded at 6.28 rad/s and 1% strain amplitude.

At high temperatures ($T > T_g$), agar molecules tended to exist in a random coil state where a predominance of the viscous character was observed ($G'' > G'$ or tan $\delta > 1$). In the early stage of the cooling ramp, the values of G' were extremely small, close to the detection limit of the equipment, and are therefore not shown. The moduli of MAE and TWE agars remained fairly constant until temperatures close to 43 °C (Note: despite the scattering of the acquired data this was the observed trend). Then, both moduli started to increase, G' increasing faster and crossing G'' at ~41–42 °C. There was consequently a sharp decrease of tan δ (inset Fig. 3), indicative of the system's elasticity gain, and was caused by the initial formation of double helices. For commercial agar, the helical organization started at lower temperatures (*i.e.* sharp decrease of tan δ at ~40 °C; inset Fig. 3). After the gelation point (tan $\delta = 1$), the elastic behavior became predominant ($G' > G''$ or tan $\delta < 1$) with the continuous increase in G' being a consequence of the side-by-side association of the helical structures to form larger aggregates which, at some point, would percolate into three-dimensional networks. G'' followed the same trend but kept much lower values. Thus, at the end of the cooling ramp, the tan δ of the three systems evolved to an asymptotic value, ~0.025, indicating comparable elasticity. Also, the G' of MAE agar (~15 kPa) was almost twice that of the TWE (~8 kPa) and clearly closer to that of the commercial agar (~19 kPa). Nonetheless, all values were around 40-times higher than the respective G'' which was in favor of 'true gels' formation, $G' \gg G''$ (Kavanagh & Ross-Murphy, 1998).

Immediately before the equilibration step, both moduli were still increasing yet at a much slower rate. Similar results

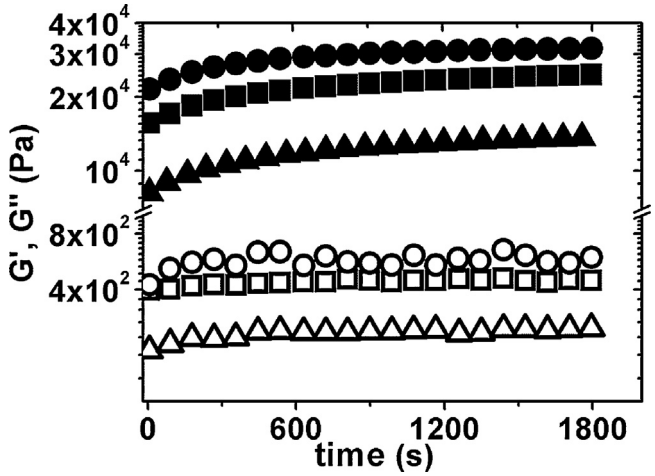

Fig. 4. Time evolution of elastic (G'; filled symbols) and viscous (G''; open symbols) moduli at 25 °C of 1.5% (w/w) agar gels recorded at 6.28 rad/s and 1% strain amplitude (MAE (■, □), TWE (▲, △) and commercial (●, ○)) agars.

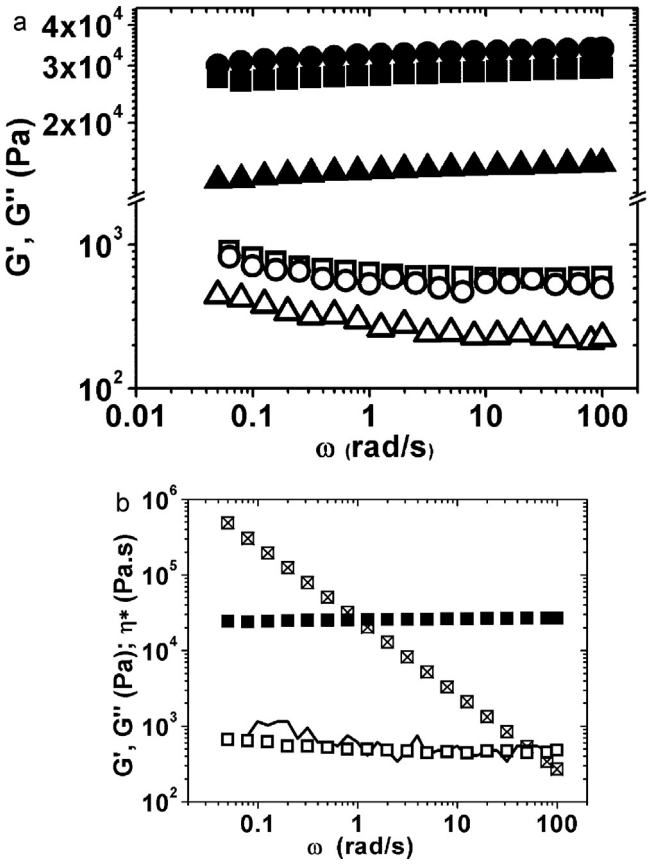

Fig. 5. Frequency dependence at 25 °C of elastic (G'; filled symbols) and viscous (G''; open symbols) moduli of 1.5% (w/w) gels of: (a) TWE (▲, △), MAE (■, □) and commercial (●, ○) agars (b) MAE agar (■, □) as well as the dynamic viscosity, η^* (open squares with cross). The solid line represents $G''(\omega)$ recalculated from $G'(\omega)$ data using the Tschoegl approximation (Eq. (1)). All measurements were recorded at 6.28 rad/s and 1% strain amplitude.

were reported by other authors when studying agarose gels (Labropoulos et al., 2001; Lahrech, Safouane, & Peyrellasse, 2005; Mohammed et al., 1998; Nordqvist & Vilgis, 2011). The curves obtained are in accordance with the view that agar gelation is a two stage kinetic process in which the limiting step is the side-by-side association of the helices (Mohammed et al., 1998). The estimated T_g values of MAE and TWE agars differed slightly (respectively, ~42.3 °C and ~40.9 °C; Table 1), and were higher than the commercial sample T_g value (~39 °C). Differences in the methoxyl contents of the polymers could explain these results (Murano, 1995). Another possible explanation could be the positive influence of the size of the polymer chains on the gelation process. In agreement with previous reports (Lahrech et al., 2005; Marinho-Soriano & Bourret, 2005; Romero et al., 2008), the higher number of potential bonding sites in MAE agar (higher M_v and 3,6-AG content) seemed to promote the aggregation of the double helices (Norziah, Foo, & Karim, 2006), with gelation occurring sooner in the cooling ramp (*i.e.* higher T_g).

The time evolution of the viscoelastic properties at 25 °C (Fig. 4), with $G' \gg G''$ throughout the entire time window, corresponds to a progressive reinforcement of the polymeric networks. It is noticeable that the MAE agar gel (G' = ~25 kPa) is more rigid than the TWE sample (G' = ~14 kPa). At the end of the time sweep, both moduli were still increasing, but slowly enough to allow the frequency sweep to be recorded with some confidence.

The 'true gel' behavior of the polymers prevailed in the recorded frequency sweeps (mechanical spectra) for the applied angular frequencies (0.05–100 rad/s in Fig. 5). Here, G' and G'' appeared practically frequency-independent which agrees well with what was found by Mohammed et al. (1998) and Labropoulos et al. (2001). There is, however, a slight monotonic increase in G' with increasing ω accompanied by a slight decrease in G'' which is typical of high molecular weight amorphous polymers (Labropoulos et al., 2001). Overall, $G''(\omega)$ values calculated by the first order approximation to Kramers-Kronig relation (Eq. (1)) were in good agreement with the measured ones (*e.g.* MAE agar in Fig. 5b), thus confirming that the data were recorded within the linear viscoelastic region of the gels (Sittikijyothin et al., 2007). Plotting the mechanical spectra in terms of $|\eta^*(\omega)|$ data (Eq. (2); *e.g.* MAE agar in Fig. 5b)) confirmed the typical 'true gel' behavior of the three agar systems (Kavanagh & Ross-Murphy, 1998) with n assuming close values, respectively, −1.01, −1.02 and −1.01 for MAE, TWE and commercial agars. The estimated dynamic consistency index K, indicated a less cohesive gel for TWE agar (20 kPa s). The MAE polymer in turn, showed values closer to the reference (31 and 37 kPa s, respectively). Accordingly, the elastic character of the systems throughout the entire frequency window followed the trend: commercial agar > MAE agar > TWE agar. For instance, taking as reference the elastic storage modulus measured at 6.28 rad/s (G_0), MAE, TWE and commercial agars showed values of respectively, ~34, ~26 and ~17 kPa. For the considered frequency, the three gel systems showed comparable elasticity, tan δ (Table 1).

Agar gels were heated from 25 to 95 °C at a very slow heating rate (0.1 °C/min) to allow the systems to equilibrate at each measured point. Results from the moduli dependence on temperature of TWE and MAE agars are illustrated in Fig. 6. The evolution with temperature of tan δ of the three agars (MAE, TWE and commercial) is presented in the inset of Fig. 6. Upon heating, the gel networks are expected to undergo a gradual transformation (*i.e.* helix-to-coil transition) until reaching again the sol state. This conformational change will occur at much higher temperatures than the gelation point due to the high stability of the formed networks (Labropoulos et al., 2001). In the beginning of the heating step, G' was much higher than G'' and remained fairly constant over a broad temperature range for the three agars, which seems to indicate that the dissociation of the aggregated helices was an equilibrium process (Mohammed et al., 1998). A sharp decrease in both moduli happened sooner for TWE agar (~56 °C) with the melting occurring around 76 °C (T_m). Subsequently, both moduli started to evolve asymptotically and, at the end of the heating period, the attained

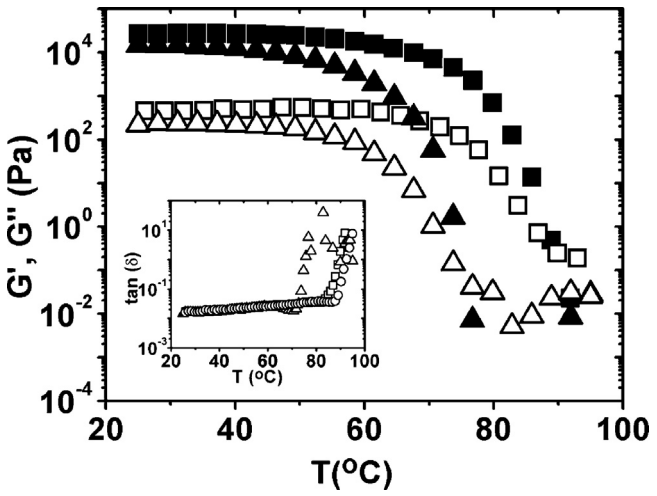

Fig. 6. Temperature dependence of elastic (G'; filled symbols) and viscous (G''; open symbols) moduli of 1.5% (w/w) agar gels/sols during heating ramp from 25 to 95 °C (MAE (■, □) and TWE (▲, △) agars). Inset figure: temperature dependence of the loss tangent of 1.5% (w/w) agar gels/sols during heating ramp from 25 to 95 °C (MAE (□), TWE (△) and commercial (○) agars). The measurements were recorded at 6.28 rad/s and 1% strain amplitude.

values of G' and G'' were respectively, 0.019 and 0.072 Pa. At this point, the system was still changing, but at a slower rate. The inverse behavior was seen for tan δ, which remained fairly constant, rising sharply after T_m (inset of Fig. 6).

Sharp decrease in the viscoelastic moduli of MAE agar started later in the heating ramp (~70 °C; Fig. 6) and consequently, the estimated T_m was significantly higher (~90 °C). Accordingly, a wider thermal hysteresis (~47 °C) was observed for the MAE sample when compared to TWE agar (~36 °C). As seen from the inset of Fig. 6, the sharp increase of tan δ of MAE agar occurred at higher temperatures, with the elasticity loss of the system evolving in a similar way to the commercial sample. This seemed consistent with the higher thermal stability of the MAE and commercial agar networks which, in turn, could be related to a positive effect of both M_v and 3,6-AG content. After the melting point, the viscous behavior became predominant ($G'' > G'$) for the three samples marking the agar transition to the sol state. For the highest temperatures, where G' and G'' assumed extremely small values (typically < 0.1 Pa), it was difficult to obtain valid data. Indeed, high variability was found in the estimated T_m ($G'' = G'$ or tan $\delta = 1$) for the MAE sample. This was not surprising in the sense that, in the temperature window where the dissociation of the junction zones takes place, the sample viscosity decreases drastically and the applied deformation can damage the gel structure to a certain point (Norziah et al., 2006). Thus, it was difficult for the rheometer to acquire valid data. Overall, a closer resemblance was found between the rheological behavior of MAE and commercial agars.

3.4. cryoSEM studies of agar gels

The 3D networks of 1.5% (w/w) MAE and TWE agar gels, whose topology depends on the type of bonding and on the conformational constraints of the polymer chains, were observed by cryoSEM imaging (Fig. 7). Rapid freezing of the gel structure reduces damage during sample preparation, particularly drying artifacts (critical in conventional SEM), thus making cryoSEM of great interest (Kaminskyj & Dahms, 2008). Agar obtained by MAE showed a more compact and regular polymeric network with well-defined pores (Fig. 7A). The pores were homogeneously distributed throughout the structure, and presented similar and smaller sizes. The denser structure obtained for MAE agar resembled that of the commercial sample (not shown) and seemed to confirm the positive contribution of molecular mass and 3,6-AG content to the assembly formation. Moreover, the attained results were in line with the higher GS value measured for MAE agar, reported as an indicator of more rigid networks (Labropoulos et al., 2001). Also, it agreed well with the higher reinforcement of the polymeric networks upon gelation recorded during the rheological measurements for MAE agar. Similar images were found by Tuvikene and co-workers (2008) for agarose gels. By contrast, agar extracted using conventional heating formed a less rigid network with the internal pores often exhibiting open irregular cavities (Fig. 7B). The larger pores of TWE agar (2–3 μm, against roughly 1 μm in MAE agar) with free dangling and thinner walls, came as no surprise and were mainly attributed to the lower 3,6-AG and molecular mass of the sample.

Overall, a very good agreement was found between the physicochemical properties, rheological and imaging studies of the polysaccharides. The higher aggregation capability of MAE agar relatively to TWE agar under comparable conditions, matched its enhanced gelling properties, as determined in texture (higher GS) and rheological (higher thermal stability and consistency of the system) measurements. These findings seemed also in favor of a positive contribution of molecular mass and 3,6-AG content to the assembly formation, rather than a direct consequence of the negative influence of the sulfate groups (*i.e.* formation of kinks

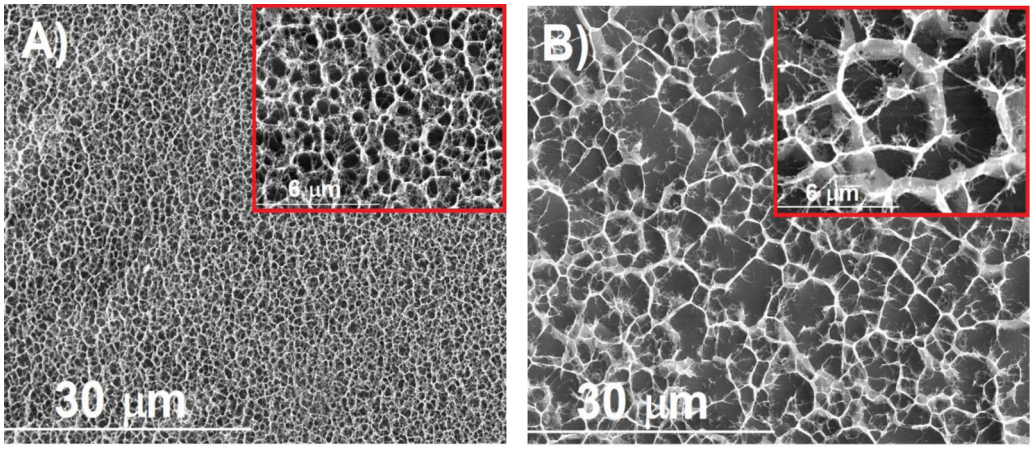

Fig. 7. Representative cryoSEM pictures obtained for 1.5% (w/w) MAE (A) and TWE (B) agar gels at 2000× and 10,000× (inset figure). The accelerating voltage was 15 kV and working-distances 15 mm in all cases.

during association of helices), which were in similar number in both agars.

4. Conclusions

MAE agar showed greater capacity for self-association than TWE agar, at comparable conditions, which seemed in accordance with its higher GS, consistency and thermal stability. At low polymer concentration, AFM images of both agars showed thin gelled layers. Depending on the cooling rate of the solutions, different structures were formed and seemed larger for MAE agar. MAE agar 3D gel network was compact and regular contrasting with a more open structure of TWE polysaccharide. Self-association seemed mostly favored by the molecular mass and 3,6-AG content. If properly controlled, non-conventional energies like microwaves could extract non-degraded agars with comparable properties to commercial ones, thermal-extracted.

Acknowledgments

This work was carried out within the line 4 of the CIQ (Centro de Investigação em Química da Universidade do Porto) research program and REQUIMTE (Laboratório Associado para a Química Verde – Tecnologias e Processos Limpos). Fundação para a Ciência e a Tecnologia (FCT) has supported REQUIMTE through Grant No. PEst-C/EQB/LA0006/2011. J. Borges and A.M.M. Sousa also gratefully acknowledge FCT for the concession of two PhD grants (SFRH/BD/47622/2008 and SFRH/BD/64315/2009, respectively). Thanks are due to Professors S. Morais and C. Matos, from GRAQ-REQUIMTE, for allowing the use of MAE apparatus, to P. Paíga for helping with the extractions and to R. Pereira and H. Abreu, from CIIMAR, for supplying the raw-material.

References

Armisen, R., & Galatas, F. (1987). Production, properties and uses of agar. In D. J. McHugh (Ed.), *Production and utilisation of products from commercial seaweeds* (pp. 1–57). FAO.

Armisen, R. (1995). Worldwide use and importance of Gracilaria. *Journal of Applied Phycology*, *7*(3), 231–243.

Arnott, S., Fulmer, A., Scott, W. E., Dea, I. C. M., Moorhouse, R., & Rees, D. A. (1974). Agarose double helix and its function in agarose-gel structure. *Journal of Molecular Biology*, *90*(2), 269–284.

Belanger, J. M. R., & Paré, J. R. J. (2006). Applications of microwave-assisted processes (MAP (TM)) to environmental analysis. *Analytical and Bioanalytical Chemistry*, *386*(4), 1049–1058.

Chan, C. H., Yusoff, R., Ngoh, G. C., & Kung, F. W. L. (2011). Microwave-assisted extractions of active ingredients from plants. *Journal of Chromatography A*, *1218*(37), 6213–6225.

Clark, A. H., & Ross-Murphy, S. B. (1987). Structural and mechanical-properties of bio-polymer gels. *Advances in Polymer Science*, *83*, 107–125.

Fishman, M. L., Chau, H. K., Cooke, P. H., & Hotchkiss, A. T. (2008). Global structure of microwave-assisted flash-extracted sugar beet pectin. *Journal of Agricultural and Food Chemistry*, *56*(4), 1471–1478.

Hurtado-Ponce, A. Q. (1992). Influence of extraction time on the rheological properties of agar from some Gracilaria species from the Philippines. *Botanica Marina*, *35*(5), 441–445.

Ikeda, S., Morris, V. J., & Nishinari, K. (2001). Microstructure of aggregated and nonaggregated kappa-carrageenan helices visualized by atomic force microscopy. *Biomacromolecules*, *2*(4), 1331–1337.

Ikeda, S., Nitta, Y., Temsiripong, T., Pongsawatmanit, R., & Nishinari, K. (2004). Atomic force microscopy studies on cation-induced network formation of gellan. *Food Hydrocolloids*, *18*(5), 727–735.

Kaminskyj, S. G. W., & Dahms, T. E. S. (2008). High spatial resolution surface imaging and analysis of fungal cells using SEM and AFM. *Micron*, *39*, 349–361.

Kavanagh, G. M., & Ross-Murphy, S. B. (1998). Rheological characterisation of polymer gels. *Progress in Polymer Science*, *23*(3), 533–562.

Labropoulos, K. C., Rangarajan, S., Niesz, D. E., & Danforth, S. C. (2001). Dynamic rheology of agar cel based aqueous binders. *Journal of the American Ceramic Society*, *84*(6), 1217–1224.

Labropoulos, K. C., Niesz, D. E., Danforth, S. C., & Kevrekidis, P. G. (2002a). Dynamic rheology of agar gels: Theory and experiments. Part I. Development of a rheological model. *Carbohydrate Polymers*, *50*(4), 393–406.

Labropoulos, K. C., Niesz, D. E., Danforth, S. C., & Kevrekidis, P. G. (2002b). Dynamic rheology of agar gels: Theory and experiments. Part II: Gelation behavior of agar sols and fitting of a theoretical rheological model. *Carbohydrate Polymers*, *50*(4), 407–415.

Lahrech, K., Safouane, A., & Peyrellasse, J. (2005). Sol state formation and melting of agar gels rheological study. *Physica A*, *358*, 205–211.

Lai, M.-F., & Lii, C. (1998). Effects of extraction conditions on structural and rheological characteristics of agar from *Pterocladia capillacea* and carrageenan from *Grateloupia filicina*. *Botanica Marina*, *41*, 223–234.

Leonelli, C., & Mason, T. J. (2010). Microwave and ultrasonic processing: Now a realistic option for industry. *Chemical Engineering and Processing*, *49*(9), 885–900.

Maaloum, M., Pernodet, N., & Tinland, B. (1998). Agarose gel structure using atomic force microscopy: Gel concentration and ionic strength effects. *Electrophoresis*, *19*(10), 1606–1610.

Marinho-Soriano, E., & Bourret, E. (2005). Polysaccharides from the red seaweed Gracilaria dura (*Gracilariales* Rhodophyta). *Bioresource Technology*, *96*(3), 379–382.

Matsuhashi, T. (1990). Agar. In P. Harris (Ed.), *Food gels* (pp. 1–51). New York: Elsevier Science Publishers.

Mohammed, Z. H., Hember, M. W. N., Richardson, R. K., & Morris, E. R. (1998). Kinetic and equilibrium processes in the formation and melting of agarose gels. *Carbohydrate Polymers*, *36*(1), 15–26.

Morris, V. J., Kirby, A. R., & Gunning, A. P. (2010). *Atomic force microscopy for biologists* (2nd ed.). London: Imperial College Press.

Murano, E. (1995). Chemical-structure and quality of agars from Gracilaria. *Journal of Applied Phycology*, *7*(3), 245–254.

Noda, S., Funami, T., Nakauma, M., Asai, I., Takahashi, R., Al-Assaf, S., et al. (2008). Molecular structures of gellan gum imaged with atomic force microscopy in relation to the rheological behavior in aqueous systems, 1. Gellan gum with various acyl contents in the presence and absence of potassium. *Food Hydrocolloids*, *22*(6), 1148–1159.

Nordqvist, D., & Vilgis, T. A. (2011). Rheological study of the gelation process of agarose-based solutions. *Food Biophysics*, *6*, 450–460.

Norziah, M. H., Foo, S. L., & Karim, A. A. (2006). Rheological studies on mixtures of agar (*Gracilaria changii*) and kappa-carrageenan. *Food Hydrocolloids*, *20*(2–3), 204–217.

Perino-Issartier, S., Zill-e-Huma, Abert-Vian, M., & Chemat, F. (2011). Solvent free microwave-assisted extraction of antioxidants from Sea Buckthorn (*Hippophae rhamnoides*) food by-products. *Food and Bioprocess Technology*, *4*(6), 1020–1028.

Pernodet, N., Maaloum, M., & Tinland, B. (1997). Pore size of agarose gels by atomic force microscopy. *Electrophoresis*, *18*(1), 55–58.

Rochas, C., & Lahaye, M. (1989). Average molecular weight and molecular weight distribution of agarose and agarose-type polysaccharides. *Carbohydrate Polymers*, *10*, 289–298.

Roesch, R., Cox, S., Compton, S., Happek, U., & Corredig, M. (2004). kappa-carrageenan and beta-lactoglobulin interactions visualized by atomic force microscopy. *Food Hydrocolloids*, *18*(3), 429–439.

Romero, J. B., Villanueva, R. D., & Montano, M. N. E. (2008). Stability of agar in the seaweed *Gracilaria eucheumatoides* (*Gracilariales* Rhodophyta) during postharvest storage. *Bioresource Technology*, *99*(17), 8151–8155.

Santana, C. M., Ferrera, Z. S., & Rodriguez, J. J. S. (2005). An environmentally friendly method for the extraction and determination of priority phenols in soils using microwave-assisted micellar extraction. *Analytical and Bioanalytical Chemistry*, *382*(1), 125–133.

Selby, H. H., & Whistler, R. L. (1993). Agar. In R. L. Whistler, & J. N. BeMiller (Eds.), *Industrial gums: polysaccharides and their derivatives* (3rd ed., pp. 87–103). San Diego, CA: Academic Press.

Sittikijyothin, W., Sampaio, P., & Gonçalves, M. P. (2007). Heat-induced gelation of beta-lactoglobulin at varying pH: Effect of tara gum on the rheological and structural properties of the gels. *Food Hydrocolloids*, *21*(7), 1046–1055.

Sousa, A. M. M., Alves, V. D., Morais, S., Delerue-Matos, C., & Gonçalves, M. P. (2010). Agar extraction from integrated multitrophic aquacultured *Gracilaria vermiculophylla*: Evaluation of a microwave-assisted process using response surface methodology. *Bioresource Technology*, *101*(9), 3258–3267.

Sousa, A. M. M., Morais, S., Abreu, M. H., Pereira, R., Sousa-Pinto, I., Cabrita, E. J., et al. (2012). Structural, physical and chemical modifications induced by microwave heating on native agar-like galactans. *Journal of Agricultural and Food Chemistry*, *60*, 4977–4985.

Souza, H. K. S, Sousa, A. M. M., Gomez, J., & Gonçalves, M. P. (2012). Complexation of WPI and microwave-assisted extracted agars with different physicochemical properties. *Carbohydrate Polymers*, *89*(4), 1073–1080.

Srogi, K. (2006). A review: Application of microwave techniques for environmental analytical chemistry. *Analytical Letters*, *39*(7), 1261–1288.

Tschoegl. (1989). *The phenomenonlogical theory of linear viscoelastic behavior: An introduction*. Berlin: Springer.

Tuvikene, R., Truus, K., Kollist, A., Volobujeva, O., Mellikov, E., & Pehk, T. (2008). Gel-forming structures and stages of red algal galactans of different sulfation levels. *Journal of Applied Phycology*, *20*, 527–535.

Villanueva, R. D., Sousa, A. M. M., Gonçalves, M. P., Nilsson, M., & Hilliou, L. (2010). Production and properties of agar from the invasive marine alga, *Gracilaria vermiculophylla* (*Gracilariales*, Rhodophyta). *Journal of Applied Phycology*, *22*(2), 211–220.